East Asian Journal on Applied Mathematics
doi: 10.4208/eajam.090217.300617a

Vol. 7, No. 3, pp. 629-642
August 2017

Hybrid Variational Model for Texture Image Restoration

Liyan Ma[1,*], Tieyong Zeng[2,3] and Gongyan Li[1]

[1] *Institute of Microelectronics of Chinese Academy of Sciences, Beijing, China.*
[2] *Department of Mathematics, Hong Kong Baptist University, Kowloon Tong, Hong Kong, China.*
[3] *HKBU Institute of Research and Continuing Education, Shenzhen Virtual University Park, Shenzhen 518057, China.*

Received 9 February 2017; Accepted (in revised version) 30 June 2017.

Abstract. The hybrid variational model for restoration of texture images corrupted by blur and Gaussian noise we consider combines total variation regularisation and a fractional-order regularisation, and is solved by an alternating minimisation direction algorithm. Numerical experiments demonstrate the advantage of this model over the adaptive fractional-order variational model in image quality and computational time.

AMS subject classifications: 65J22, 65K10, 68U10

Key words: Image deblurring, total variation, fractional-order regularisation.

1. Introduction

Image restoration is a crucial pre-processing step for many applications, and it is widely used in computer vision. In order to improve image quality, various models have been proposed recently. Image restoration is a typical inverse problem that can be viewed as an estimation problem. Here we focus on recovering images corrupted by a spatially-invariant blur and a Gaussian noise. The image degradation model can be represented by the equation

$$g = Af + n\,, \tag{1.1}$$

where $f \in \mathbb{R}^{N_y \times N_x}$ is a clear image, $g \in \mathbb{R}^{N_y \times N_x}$ is the observed image, A is a known linear operator from $\mathbb{R}^{N_y \times N_x}$ to $\mathbb{R}^{N_y \times N_x}$, and n represents an additive Gaussian noise.

Inverse problems in image processing are typically ill-posed. A common strategy to tackle such problems is a variational approach, which we also use here. There are two phases in a variational model — viz. regularisation and data fidelity. The regularisation plays an important role in inverse problems, and is used to reduce the space of possible

*Corresponding author. *Email addresses:* maliyan@ime.ac.cn (L. Ma), zeng@hkbu.edu.hk (T. Zeng), ligongyan@ime.ac.cn (G. Li)

 ©2017 Global-Science Press

https://doi.org/10.4208/eajam.090217.300617a Published online by Cambridge University Press

solutions. A proper regularisation has to capture the most important properties of an image and improve the visual quality of the recovered image. Over the past decades, many works deal with the regularisation procedure — cf. Refs. [7, 13, 17, 24, 36, 37]. A common approach used in inverse problems is the Tikhonov L_2-norm regularisation [35] that effectively removes the noise, but since it over-smooths image edges Rudin *et al.* [32] proposed an L_1-norm regularisation called total variation (TV) regularisation that is convex, preserves sharp edges and allows the use of powerful optimisation methods [3, 5, 22, 41]. The TV regularisation has been successfully applied in applications [11, 18, 25, 40] such as image restoration, image segmentation, motion estimation, and image reconstruction. However, it does not preserve fine details and has a staircase effect caused by the model assumption that the underlying image is piecewise constant, which in most cases does not hold.

To overcome disadvantages of the TV regularisation, several other regularisation functionals have been considered recently. Chambolle & Lions [10] introduced second order derivatives; Berkels *et al.* [4] studied an anisotropic regularisation based on the local structure of the image; a locally varying regularisation weight was used by Grasmair [21] in locally adaptive TV regularisation; Lou *et al.* [23] examined the image gradient and proposed a weighted difference of anisotropic and isotropic TV regularisation; and for a better balance between noise removal and edge preservation, You & Kaveh [42] introduced a fourth-order PDE model. Bredies *et al.* [6] proposed a total generalised variation (TGV) regularisation, which is a version of the TV regularisation involving higher-order derivatives that preserves piecewise polynomial intensities and sharp edges, suppressing the staircase effect and improving the visual image quality. Setzer *et al.* [33] reduced the staircasing artifacts of the restoration results in Chambolle & Lions [10] by an infimal convolutions modification. Bai & Feng [2] developed a fractional-order anisotropic diffusion model as a replacement for second order and fourth-order anisotropic diffusion equations; and using the regularisation parameter selection method of Ref. [19], Zhang *et al.* [46] proposed an adaptive fractional-order multi-scale method for image denoising. To fix texture deblurring, Chan *et al.* [12] introduced a spatially adaptive fractional order TV regularisation term with different fractional orders for different texture regions, which produces very promising results on texture images but finding the texture map is not easy. Regularisation with different fractional orders utilises many neighbourhood pixels which can cause unexpected errors, especially for pixels on the boundary between different textures.

While computing the partial derivatives in fractional-order regularisation, the many neighbourhood pixels involved effectively collect texture information — and here we focus on texture image deblurring based on a fractional order TV regularisation. To overcome the limitation of the method in Ref. [12], we use an hybrid variational model that combines TV regularisation and fractional order TV regularisation, so time consuming texture map calculations are avoided. Experimental results demonstrate the efficiency of this approach, in both the quality of image restoration and computational time. In Section 2, we recall the concept of fractional-order regularisation, and our algorithm is introduced in Section 3. Section 4 contains numerical results demonstrating the algorithm efficiency, and our concluding remarks are in Section 5.

https://doi.org/10.4208/eajam.090217.300617a Published online by Cambridge University Press

2. Fractional-Order Regularisation

Given an image f, TV regularisation [32] is defined by the functional

$$\|\nabla f\|_1 := \sum_{i,j} \sqrt{(D_x f)_{i,j}^2 + \left(D_y f\right)_{i,j}^2}\,, \tag{2.1}$$

where $(D_x f)_{i,j}$ and $\left(D_y f\right)_{i,j}$ are partial derivatives of f at the location (i,j). In general, the information from two pixels is needed to calculate a discrete derivative in the TV regularisation , so the procedure does not require too much local information. The total fractional-order regularisation is defined by another functional

$$\|\nabla^\alpha f\|_1 := \sum_{i,j} \sqrt{\left(D_x^\alpha f\right)_{i,j}^2 + \left(D_y^\alpha f\right)_{i,j}^2}\,, \tag{2.2}$$

where α is a real number and $(D_x^\alpha f)_{i,j}$ and $(D_y^\alpha f)_{i,j}$ are the x and y directional fractional-order derivatives of f at the location (i,j) — cf. Refs. [12, 14, 15, 44]. There are various definitions for fractional-order derivatives, but we prefer to use the Grunwald-Letnikov definition [27, 30] here — viz. for a function f, its x and y-directional derivatives of the order α at the location (i,j) are defined as

$$\left(D_x^\alpha f\right)_{i,j} := \sum_{m=0}^{M-1} c_m^\alpha f_{i-m,j}\,, \qquad \left(D_y^\alpha f\right)_{i,j} := \sum_{m=0}^{M-1} c_m^\alpha f_{i,j-m}\,, \tag{2.3}$$

where $M > 0$ is the number of pixels used in calculation of the discrete derivative,

$$c_m^\alpha := (-1)^m \begin{pmatrix} \alpha \\ m \end{pmatrix} = (-1)^m \frac{\Gamma(\alpha+1)}{\Gamma(m+1)\Gamma(\alpha-m+1)}\,,$$

and Γ denotes the Gamma function. We take $M = 8$, $\alpha \in (1,2)$ and recall the coefficients c_m^α can be calculated by the recursive relations

$$c_0^\alpha = \begin{pmatrix} \alpha \\ 0 \end{pmatrix} = 1\,, \qquad c_m^\alpha = \left(1 - \frac{\alpha+1}{m}\right) c_{m-1}^\alpha\,, \qquad m = 1, 2, \cdots. \tag{2.4}$$

If $\alpha = 1$, then for all $m > 1$ the coefficients c_m^1 are equal to zero such that $D_x^1 f$ and $D_y^1 f$ are the usual discrete partial derivatives so (2.2) becomes the TV regularisation. Analogously, for $\alpha = 2$ one obtains the common discrete second-order derivatives. Moreover, it is easily seen that for fixed α the coefficients c_m^α rapidly tend to zero as m increases. As noted in Ref. [12], the fractional derivatives (2.3) of different order α correspond to different high-pass filters. For a large α the cutoff frequency is lower, so a larger number of texture regions is well preserved (the nonlocal nature of the fractional-order regularisation better preserves the detail.)

In natural images, there are both smooth regions and texture regions with different frequencies, so Chan *et al.* [12] used an adaptive fractional order regularisation for the

https://doi.org/10.4208/eajam.090217.300617a Published online by Cambridge University Press

texture regions and TV regularisation for the smooth regions. The regularisation is defined by

$$\lambda_{i,j}\sqrt{\left(D_x^{\alpha_{i,j}}f\right)_{i,j}^2+\left(D_y^{\alpha_{i,j}}f\right)_{i,j}^2+\beta}\,, \tag{2.5}$$

where $\beta>0$ is a constant, while the $\lambda_{i,j}>0$ are related to the parameters $\alpha_{i,j}$ and responsible for coordination between the regularisation and data-fidelity terms. In practice, Chan *et al.* [12] segmented an image into non-texture and texture classes. The texture classes have been further subdivided depending on the texture values and for each region its own fractional-order regularisation was used. This algorithm provides a good texture retrieval, but finding the texture map for natural images is difficult. The parameter β influences the behaviour of the regularisation (2.5) and may cause over-smoothness of sharp features. In addition, the use of neighbourhood pixels in the fractional order regularisation may produce unexpected errors, especially on the boundary of regions with different textures.

3. Proposed Model

The aim of this work is to introduce an algorithm which avoids weaknesses of the approach of Chan *et al.* [12]. As mentioned, for deblurring of texture images we use an hybrid model based on the TV regularisation and a fractional-order regularisation. Recall that image decomposition plays an important role in image processing. Meyer studied this problem for cartoon + texture images and proposed a way for its solution [26]. An image is usually decomposed into the sum of cartoon and texture. The cartoon part can be represented by a piecewise smooth function, and the texture part is an oscillatory pattern. Since decomposition allows a better handling of texture images, it has often been used in variational models or wavelet analysis — cf. Refs. [16, 19, 28, 29, 31, 38, 43]. On the other hand, Buades *et al.* [8] presented a filter version of image decomposition. Here we also employ the cartoon + texture decomposition together with a fractional-order regularisation when considering the deblurring problem.

The proposed model is given by

$$\min_{u,v}\|\nabla u\|_1+\beta\,\|\nabla^{\alpha}v\|_1+\frac{\lambda}{2}\left\|A(u+v)-g\right\|_2^2, \tag{3.1}$$

with fixed positive numbers β and λ. The underlying image f consists of the carton and texture parts u and v, so that

$$f=u+v\,.$$

In our approach, the cartoon and texture parts u and v are penalised by the TV regularisation (favouring piecewise-constant solutions) and the fractional-order regularisation (favouring fine-scale feature preservation), respectively.

In the presence of two unknown variables, we apply an alternating minimisation direc-

https://doi.org/10.4208/eajam.090217.300617a Published online by Cambridge University Press

tion approach to the functional (3.1). The algorithm scheme is given by

$$u^{n+1} = \arg\min_u \|\nabla u\|_1 + \frac{\lambda}{2}\left\|A(u+v^n) - g\right\|_2^2,$$
$$v^{n+1} = \arg\min_v \beta\,\|\nabla^\alpha v\|_1 + \frac{\lambda}{2}\left\|A(u^{n+1}+v) - g\right\|_2^2, \tag{3.2}$$

and the image can be recovered as

$$f^{n+1} = u^{n+1} + v^{n+1}.$$

Note that the application of traditional TV deblurring schemes to the first minimisation problem in (3.2) meets difficulties because of non-differentiability of the TV regularisation. However, a number of effective methods have been developed recently — e.g. the variable splitting method [1], Bregman method [20], alternating direction method of multipliers [39], dual methods [9] and primal-dual methods [11]. The relationships between some of these methods are discussed in Ref. [34], and here we employ the first-order primal-dual algorithm [11].

Introducing a dual variable p, we get

$$\|\nabla u\|_1 = \sup_{p\in U} -\langle u, \operatorname{div} p\rangle - \delta_P\,,$$

where $U = \mathbb{R}^{N_y\times N_x}\times\mathbb{R}^{N_y\times N_x}$, δ_P is the indicator function of the set $P = \{p\in U; \|p\|_\infty \le 1\}$, and $\operatorname{div} := -\nabla^*$ is the divergence operator. The primal-dual formulation of the first minimisation problem in (3.2) reduces to finding the term

$$\min_u \max_{p\in U} -\langle u, \operatorname{div} p\rangle - \delta_P + \frac{\lambda}{2}\left\|A(u+v^n) - g\right\|_2^2. \tag{3.3}$$

Applying the first-order primal-dual algorithm [11] to (3.3), we obtain

$$p^{k+1} = \arg\min_p \left\langle \bar{u}^k, \operatorname{div} p\right\rangle + \delta_P + \frac{1}{2t_p}\left\|p-p^k\right\|_2^2,$$
$$u^{k+1} = \arg\min_u -\left\langle u, \operatorname{div} p^{k+1}\right\rangle + \frac{\lambda}{2}\left\|A(u+v^n) - g\right\|_2^2 + \frac{1}{2t_u}\left\|u-u^k\right\|_2^2,$$
$$\bar{u}^{k+1} = 2u^{k+1} - u^k\,,$$

where t_p and t_u are positive constants and k is the iteration number. The sub-optimisation problem for updating p is equivalent to determining the minimum

$$\min_p -\left\langle \nabla\bar{u}^k, p\right\rangle + \delta_P + \frac{1}{2t_p}\left\|p-p^k\right\|_2^2,$$

with the following update rules for p and u:

$$p^{k+1} = \frac{p^k + t_p\cdot\nabla\bar{u}^k}{\max\left(1, \left|p^k + t_p\cdot\nabla\bar{u}^k\right|\right)}, \tag{3.4}$$

$$u^{k+1} = \frac{u^k - t_u\cdot\left(-\operatorname{div} p^{k+1} + \lambda A^*(Av^n - g)\right)}{I + t_u\lambda A^*A}. \tag{3.5}$$

https://doi.org/10.4208/eajam.090217.300617a Published online by Cambridge University Press

The second minimisation problem in (3.2) is the texture component calculation. We recall that Zhang & Chen [45] showed that the fractional-order regularisation term is convex, so the second minimisation functional in (3.2) is convex and we can use the first-order primal-dual method. Rewriting the total fractional-order regularisation, we get

$$\|\nabla^{\alpha} v\|_1 = \sup_{q\in U} -\langle v, \mathrm{div}^{\alpha} q\rangle - \delta_Q \,,$$

where q is a dual variable, δ_Q is the indicator function of the set $Q = \{q \in U; \|q\|_\infty \le \beta\}$, and $\mathrm{div}^{\alpha} := -(\nabla^{\alpha})^*$. The primal-dual formulation of the second minimisation problem in (3.2) becomes

$$\min_{v}\max_{q\in U} -\langle v, \mathrm{div}^{\alpha} q\rangle - \delta_Q + \frac{\lambda}{2}\left\|A(u^{n+1}+v)-g\right\|_2^2 \,. \tag{3.6}$$

Applying again the first-order primal-dual algorithm [11] to (3.6), we obtain

$$\begin{aligned}
q^{k+1} &= \arg\min_{q} \left\langle \bar{v}^k, \mathrm{div}^{\alpha} q\right\rangle + \delta_Q + \frac{1}{2t_q}\left\|q-q^k\right\|_2^2 \,,\\
v^{k+1} &= \arg\min_{v} -\left\langle v, \mathrm{div}^{\alpha} q^{k+1}\right\rangle + \frac{\lambda}{2}\left\|A(u^{n+1}+v)-g\right\|_2^2 + \frac{1}{2t_v}\left\|v-v^k\right\|_2^2 \,,\\
\bar{v}^{k+1} &= 2v^{k+1}-v^k \,,
\end{aligned}$$

where t_q and t_v are positive constants. If q denotes the vector $[q_1, q_2]$, then

$$-\mathrm{div}^{\alpha} q^{k+1} = \sum_{m=0}^{M-1} c_m^{\alpha} (q_1^{k+1})_{i+m,j} + \sum_{m=0}^{M-1} c_m^{\alpha} (q_2^{k+1})_{i,j+m} \,;$$

and similarly to the solution of the first minimisation problem, the update rules for q and v are

$$q^{k+1} = \frac{q^k + t_q \cdot \nabla^{\alpha}\bar{v}^k}{\max\left(\beta, \left|q^k + t_q \cdot \nabla^{\alpha}\bar{v}^k\right|\right)} \,, \tag{3.7}$$

$$v^{k+1} = \frac{v^k - t_v \cdot \left(-\mathrm{div}\, q^{k+1} + \lambda A^*\left(Au^{n+1}-g\right)\right)}{I + t_v \lambda A^* A} \,. \tag{3.8}$$

Finally, the algorithm we use for deblurring of texture images can therefore be summarised in Algorithm 1.

4. Experimental Results

In this section, we demonstrate the efficiency of our algorithm and compare it with the AF algorithm [12], the TV based model [11], the TGV model using the first and second derivatives, the total fractional-order variation (TFV) model [15], and with the ADMGB algorithm [29] based on image decomposition. For the solution of the TFV model, we use the

https://doi.org/10.4208/eajam.090217.300617a Published online by Cambridge University Press

Algorithm 1 Algorithm for image deblurring on texture images.

Initialisation: $\bar{u}^0 = g$, $u^0 = g$, $p^0 = \vec{0}$, $q^0 = \vec{0}$, $\lambda, \alpha, \beta, t_u, t_p, t_v, t_q$.
Output: $f^{n+1} = u^{n+1} + v^{n+1}$.
for $n = 0:, 1, \cdots, N_O$ **do**
  for $k = 0, 1, \cdots, N_I$ **do**
    Compute p^{k+1} using (3.4);
    Compute u^{k+1} using (3.5);
    $\bar{u}^{k+1} = 2u^{k+1} - u^k$;
  end for
  $u^{n+1} = u^{k+1}$;
  for $k = 0, 1, \cdots, N_I$ **do**
    Compute q^{i+1} using (3.7);
    Compute v^{k+1} using (3.8);
    $\bar{v}^{k+1} = 2v^{k+1} - v^k$;
  end for
  $v^{n+1} = v^{k+1}$;
end for

primal-dual algorithm from Ref. [11]. All images are blurred by a 3×3 Gaussian blur with standard deviation 1.5, generated by the MATLAB function 'fspecial'. In all experiments, we set $t_p = t_q = t_u = t_v = 1/4$, $N_I = 1$. The remaining parameters were empirically tuned to improve the performance of the algorithm. In the AF algorithm, we used the code provided by the authors, where every image is partitioned into fours regions — viz. three texture regions and a non-texture region. The corresponding fractional orders were set to be $1.9, 1.8, 1.7, 1.0$. The peak-signal-to-noise ratio (PSNR) that measures the quality of the restored images was defined as

$$PSNR = 20 \log_{10} \frac{255}{\frac{1}{mn}\left\|\tilde{f} - f\right\|_F}, \tag{4.1}$$

where f and $\tilde{f}$ denote the true and recovered images, respectively. The stopping criterion reflected the relative difference between successive iterations of the restored image (RDS) — cf. Ref. [11, 41], defined by

$$RDS\left(f^{n+1}, f^n\right) = \frac{\left\|f^{n+1} - f^n\right\|_2}{\|f^{n+1}\|_2}.$$

Thus the algorithm stops when $RDS(f^{n+1}, f^n) < \varepsilon$, and we chose $\varepsilon := 10^{-4}$.

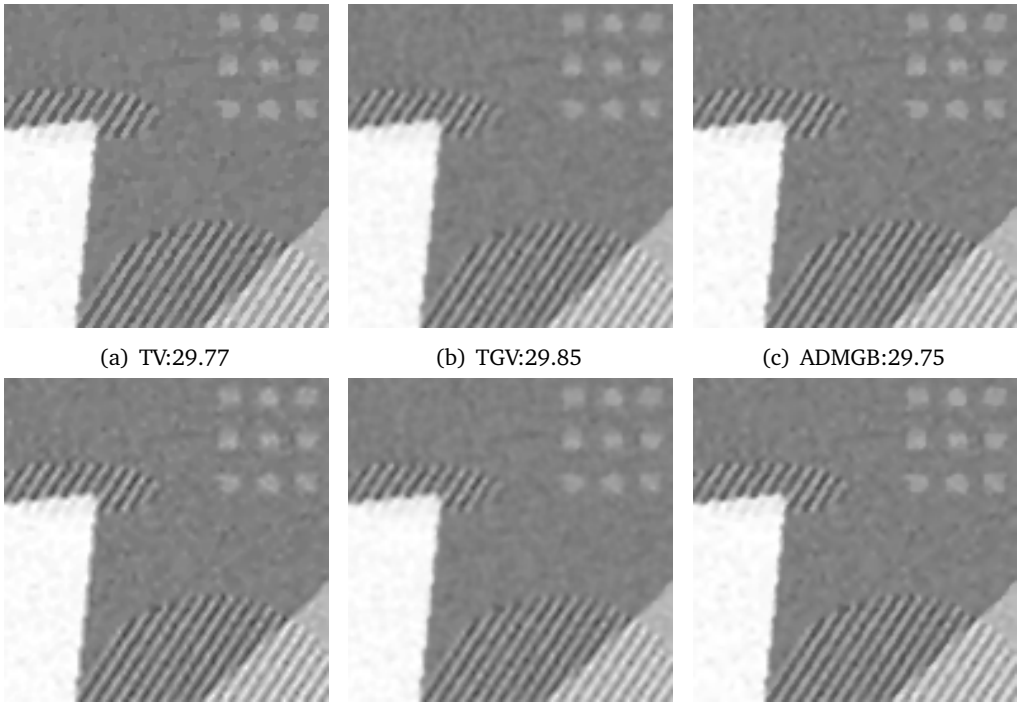
In the deblurring of test images corrupted by blur and 5% Gaussian noise, the regularisation parameters for the above mentioned classes in the AF algorithm were $0.2, 0.2, 0.2$ and 0.5, and The fractional order and the regularisation parameter in the TFV algorithm 1.8 and 0.8, respectively. The parameters in the TV-based algorithm, TGV and ADMGB were tuned to improve the results. In our algorithm, we set $\alpha = 1.8$, $\lambda = 0.5$ and Fig. 2 shows

https://doi.org/10.4208/eajam.090217.300617a Published online by Cambridge University Press



(a) Test (b) Barbara (c) Lena (d) Man

Figure 1: Original images.



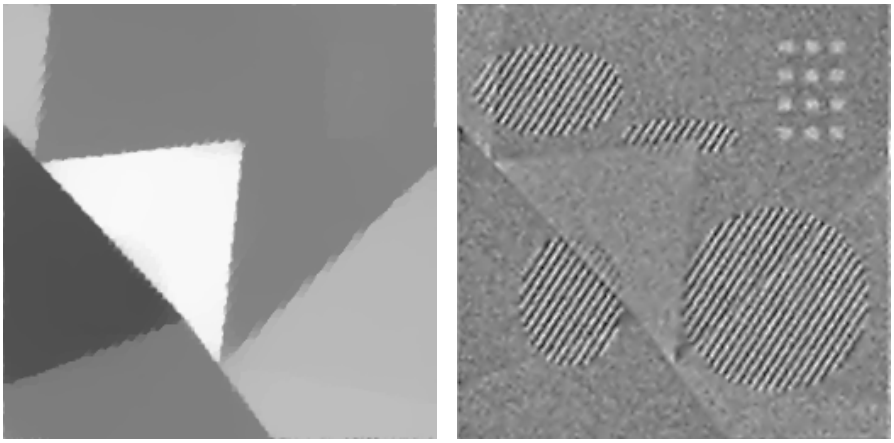
(a) TV:29.77 (b) TGV:29.85 (c) ADMGB:29.75

(d) TFV:29.98 (e) AF:30.12 (f) Our:30.35

Figure 2: A zoomed region of the restored test image corrupted by blur and 5% Gaussian noise.

the results. The test image regions have different smoothness and texture, and the TFV provides a better texture description than the TV regularisation. TGV also produces better results than TV regularisation. ADMGB uses image decomposition, but it does not perform well since the constraint for the texture part provides unsatisfactory texture information. The AF algorithm delivers a better result due to a spatially adaptive fractional-order regularisation term. Nevertheless, our algorithm gives the best recovery, since for the cartoon and texture components it respectively uses TV and a fractional-order regularisations. Fig. 3 presents two components of the recovered image. It is obvious that the cartoon component is rather smooth and the other one is composed of textures.

https://doi.org/10.4208/eajam.090217.300617a Published online by Cambridge University Press



(a) u (b) v

Figure 3: The cartoon (left) and texture (right) parts of the recovered blurred test image.



(a) TV:21.76 (b) TGV:21.90 (c) ADMGB:21.85

(d) TFV:22.01 (e) AF:21.76 (f) Our:22.06

Figure 4: A zoomed region of the restored image Barbara corrupted by blur and 5% Gaussian noise.

For the degraded images Barbara, Lena and Man commonly used in image processing, Table 1 contains PSNR values of the images recovered by six algorithms, and Figs. 4, 5 and 6 show some of the recovered images. For the image Barbara containing both regular textures

https://doi.org/10.4208/eajam.090217.300617a Published online by Cambridge University Press



(a) TV:33.35 (b) TGV:33.61 (c) ADMGB:33.22

(d) TFV:33.03 (e) AF:33.10 (f) Our:33.44

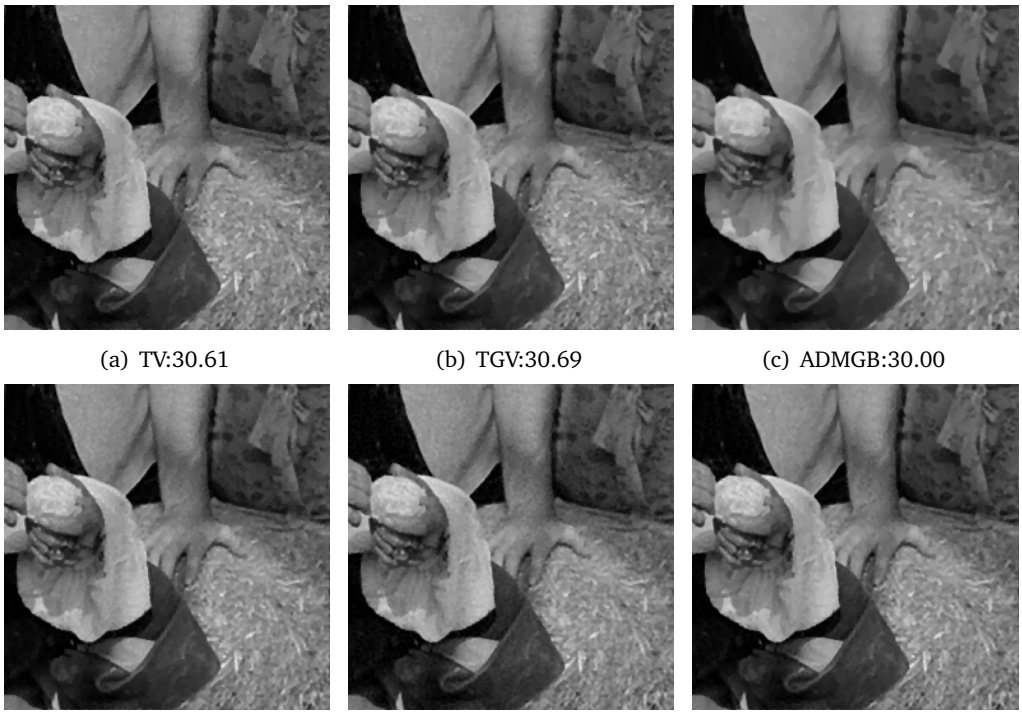
Figure 5: A zoomed region of the restored image Lena corrupted by blur and 5% Gaussian noise.

Table 1: PSNR(dB) for the images corrupted by blur and Gaussian noise, with the noise levels 5% and 10%.

	0.05				0.1			
	Test	Barbara	Lena	Man	Test	Barbara	Lena	Man
TV	29.77	21.76	33.35	30.61	27.38	20.78	31.38	28.86
TGV	29.85	21.90	33.61	30.69	27.43	20.76	31.60	28.95
ADMGB	29.75	21.85	33.22	30.00	27.49	20.69	31.06	28.42
TFV	29.98	22.01	33.03	30.45	27.57	20.83	31.06	28.68
AF	30.12	21.76	33.10	30.18	27.66	20.81	30.85	28.38
Ours	30.35	22.06	33.44	30.77	27.71	20.85	31.44	28.95

and smooth regions, the best results are provided by TFV and our algorithm. The main component of the image Lena is a smooth region, so the superiority of the fractional-order regularisation over the TV is reduced, and the TGV that preserves piecewise polynomial intensities produces the best results. The image Man has various irregular textures, so the texture map is not well defined and the AF method does not work properly. However, our algorithm processes the cartoon and texture parts separately in a robust performance.

https://doi.org/10.4208/eajam.090217.300617a Published online by Cambridge University Press



(a) TV:30.61 (b) TGV:30.69 (c) ADMGB:30.00

(d) TFV:30.45 (e) AF:30.18 (f) Our:30.77

Figure 6: A zoomed region of the restored image Man corrupted by blur and 5% Gaussian noise.

Moreover, in comparison to the AF method our approach not only provides better quality of the recovered images but also requires less computational cost. For example, the processing of a 255×255 test image takes about 8.3 seconds, while the AF method needs 57.3 seconds for the same operation. For the 512×512 Man image our method requires about 30.2 seconds, while the AF method needs 236.2 seconds. All of the numerical experiments were conducted on a PC equipped with a 2.70 GHz CPU, in the Matlab 7.12 (R2011a) environment.

5. Conclusion

We have presented an effective and efficient algorithm for restoration of blurred texture images with Gaussian noise. The proposed model takes advantage of the cartoon+texture decomposition model by using total variation regularisation and fractional-order regularisation to constrain the cartoon and texture parts, respectively. The total variation regularisation preserves the strong edges, while the fractional-order regularisation preserves the details of the image. We used an alternating minimisation direction algorithm to solve the model. Our numerical experiments demonstrate the efficiency of the algorithm and a higher image restoration quality.

https://doi.org/10.4208/eajam.090217.300617a Published online by Cambridge University Press

Acknowledgments

The authors thank R.H. Chan, A. Lanza, S. Morigi and F. Sgallari for providing the code of [12] and Wenxing Zhang for the code of Ref. [29]. The authors also thank the anonymous referees for their extremely useful suggestions that improved the manuscript. The research is supported by the National Natural Science Foundation of China (No. 61402462, 11271049), RGC 211911, 12302714, and RFGs of HKBU.

References

[1] M.V. Afonso, J.M. Bioucas-Dias and M.A.T. Figueiredo, *Fast image recovery using variable splitting and constrained optimization*, IEEE Trans. Image Process. **19**, 1057-7149 (2010).
[2] J. Bai and X.C. Feng, *Fractional-order anisotropic diffusion for image denoising*, IEEE Trans. Image Process. **16**, 2492-2502 (2007).
[3] A. Beck and M. Teboulle, *A fast iterative shrinkage-thresholding algorithm for linear inverse problems*, SIAM J. Imaging Sci. **2**, 183-202 (2009).
[4] B. Berkels, M. Burger, M. Droske, O. Nemitz and M. Rumpf, *Cartoon extraction based on anisotropic image classification vision, modeling, and visualization*, Vision, Modeling, and Visualization, pp. 293-300, Akademische Verlagsgesellschaft (2006).
[5] S. Boyd and L. Vandenberghe, *Convex Optimization*, Cambridge University Press (2004).
[6] K. Bredies, K. Kunisch and T. Pock, *Total generalized variation*, SIAM J. Imaging Sci. **3**, 492-526 (2010).
[7] A. Buades, B. Coll and J.M. Morel, *A review of image denoising algorithms, with a new one*, Multiscale Model. Simul. **4**, 490-530 (2005).
[8] A. Buades, T.M. Le, J.M. More and L. Vese, *Fast cartoon+texture image filters*, IEEE Trans. Image Process. **19**, 1978-1986 (2010).
[9] A. Chambolle, *An algorithm for total variation minimization and applications*, J. Math. Imag. Vis. **20**, 89-97 (2004).
[10] A. Chambolle and P.L. Lions, *Image recovery via total variation minimization and related problems*, Numer. Math. **76**, 167-188 (1997).
[11] A. Chambolle and T. Pock, *A first-order primal-dual algorithm for convex problems with applications to imaging*, J. Math. Imaging Vis. **40**, 120-145 (2011).
[12] R.H. Chan, A. Lanza, S. Morigi and F. Sgallari, *An adaptive strategy for the restoration of textured images using fractional order regularization*, Numer. Math. Theor. Meth. Appl. **6**, 276-296 (2013).
[13] T. Chan and H.M. Zhou, *Total variation wavelet thresholding*, J. Sci. Comput. **32**, 315-341 (2007).
[14] D. Chen, Y. Chen and D. Xue, *Three fractional-order TV-l2 models for image denoising*, J. Comput. Inform. Syst. **9**, 4773-4780 (2013).
[15] D. Chen, Y. Chen and D. Xue, *Fractional-order total variation image denoising based on proximity algorithm*, Appl. Math. Comput. **257**, 537-545 (2015).
[16] I. Daubechies and G. Teschke, *Variational image restoration by means of wavelets: Simultaneous decomposition, deblurring, and denoising*, Appl. Comput. Harmon. A. **19**, 1-16 (2005).
[17] B. Dong, H. Ji, J Li, Z. Shen and Y. Xu, *Wavelet frame based blind image inpainting*, Appl. Comput. Harmon. A. **32**, 268-279 (2012).
[18] Y. Dong, M. Hintermüler and M. Neri, *An efficient primal-dual method for L^1TV image restoration*, SIAM J. Imag. Sci. **2**, 1168-1189 (2009).

https://doi.org/10.4208/eajam.090217.300617a Published online by Cambridge University Press

[19] G. Gilboa, N. Sochen and Y.Y. Zeevi, *Variational denoising of partly textured images by spatially varying constraints*, IEEE Trans. Image Process. **15**, 2281-2289 (2006).
[20] T. Goldstein and S. Osher, *The split Bregman algorithm for L1 regularized problems*, SIAM J. Imag. Sci. **2**, 323-343 (2009).
[21] M. Grasmair, *Locally adaptive total variation regularisation*, in *Scale Space and Variational Methods in Computer Vision*, X. Tai, K. Morken, O.M. Lysaker and K. Lie (Eds.), pp. 331-342, Springer (2009).
[22] X. Guo, F. Li and M.K. Ng, *A fast l^1-TV algorithm for image restoration*, SIAM J. Sci. Comput. **31**, 2322-2341 (2009).
[23] Y. Lou, T. Zeng, S. Osher and J. Xin, *A weighted difference of anisotropic and isotropic total variation model for image processing*, SIAM J. Imag. Sci. **8**, 1798-1823 (2015).
[24] Y. Lou, X. Zhang, S. Osher and A. Bertozzi, *Image recovery via nonlocal operators*, J. Sci. Comput. **42**, 185-197 (2010).
[25] L. Ma, M. Ng, J. Yu and T. Zeng, *Efficient box-constrained TV-type-l1 algorithms for restoring images with impulse noise*, J, Comput. Math. **31**, 249-270 (2013).
[26] Y. Meyer, *Oscillating Patterns in Image Processing and in Some Nonlinear Evolution Equations. The Fifteenth Dean Jacquelines B. Lewis Memorial Lectures*, American Mathematical Society (2001).
[27] K.S. Miller and B. Ross, *An Introduction to the Fractional Calculus and Fractional Differential Equations*, Wiley Interscience (1993).
[28] M. Ng, H. Ngan, X. Yuan and W. Zhang, *Patterned fabric inspection and visualization by the method of image decomposition*, IEEE Trans. Aotum. Sci. Eng. **11**, 943-947 (2013).
[29] M. Ng, X. Yuan and W. Zhang, *A coupled variational image decomposition and restoration model for blurred cartoon-plus-texture images with missing pixels*, IEEE Trans. Image Process. **22**, 2233-2246 (2013).
[30] K.B.A. Oldham and J.A. Spanier, *The Fractional Calculus: Theory and Applications of Differentiation and Integration to Arbitrary Order*, Dover (2006).
[31] S. Osher, A. Sole and L. Vese, *Image decomposition and restoration using total variation minimization and the H1*, Multiscale Modeling & Simulation **1**, 349-370 (2003).
[32] L. Rudin, S. Osher and E. Fatemi, *Nonlinear total variation based noise removal algorithms*, Physica D **60**, 259-268 (1992).
[33] S. Setzer, G. Steidl and T. Teuber, *nfimal convolution regularizations with discrete L1-type functionals*, Comm. Math. Sci. **9**, 797-872 (2011).
[34] X.-C. Tai and C. Wu, *Augmented Lagrangian method, dual methods and split Bregman iteration for ROF model*, SSVM 2009, LNCS 5567, **42**, pp. 502-513, Springer (2009) .
[35] A. Tikhonov and V. Arsenin, *Solution of Ill-Posed Problems*, Winston and Sons (1977).
[36] W. Wang and M.K. Ng, *On algorithms for automatic deblurring from a single image*, J. Comput. Math. **30**, 80-100 (2012).
[37] Y-W. Wen, M.K. Ng and Y. Huang, *Efficient total variation minimization methods for color image restoration*, IEEE Trans. Image Process. **17**, 2081-2088 (2008).
[38] L. Vese and S. Osher, *Modeling textures with total variation minimization and oscillating patterns in image processing*, J. Sci. Computing **19**, 553-572 (2003).
[39] C. Wu, J. Zhang and X.-C. Tai, *Augmented lagrangian method for total variation restoration with non-quadratic fidelity*, Inverse Problems Imag. **5**, 237-261 (2011).
[40] F. Yang, K. Chen and B. Yu, *Homotopy curve tracking for total variation image restoration*, J. Comput. Math. **30**, 177-196 (2012).
[41] J. Yang, Y. Zhang and W. Yin, *An efficient TVL1 algorithm for deblurring multichannel images corrupted by impulsive noise*, SIAM J. Sci. Comput. **31**, 2842-2865 (2009).

https://doi.org/10.4208/eajam.090217.300617a Published online by Cambridge University Press

[42] Y.L. You and M. Kaveh, *Fourth-order partial differential equations for noise removal*, IEEE Trans. Image Process. **9**, 1723-1730 (2000).
[43] T. Zeng, X. Li and M. Ng, *Alternating minimization method for total variation based wavelet shrinkage model*, Commun. Comput. Phys. **8**, 976-994 (2010).
[44] X. Zhang, M. Burger, X. Bresson and S. Osher, *Bregmanized nonlocal regularization for deconvolution and sparse reconstruction*, SIAM J. Imag. Sci. **3**, 253-276 (2010).
[45] J. Zhang and K. Chen, *A total fractional-order variation model for image restoration with nonhomogeneous boundary conditions and its numerical solution*, SIAM J. Imag. Sci. **8**, 2487-2518 (2015).
[46] J. Zhang, Z. Wei and L. Xiao, *Adaptive fractional-order multi-scale method for image denoising*, SIAM J. Imag. Sci. **43**, 39-49 (2012).

https://doi.org/10.4208/eajam.090217.300617a Published online by Cambridge University Press